

# The combined deterministic stochastic subspace based system identification in buildings

Pelin Gundes Bakir\*

Department of Civil Engineering, Istanbul Technical University, Adnan Saygun Cad.,  
Selin apt. No:15-9, D:13, Ulus, Besiktas, Istanbul, Turkey

(Received November 4, 2009, Accepted December 28, 2010)

**Abstract.** The Combined Deterministic Stochastic Subspace based System Identification Technique (CDSSSIT) is a powerful input-output system identification technique which is known to be always convergent and numerically stable. The technique determines a Kalman state sequence from the projection of the output-input data. The state space matrices are determined subsequently from this Kalman state sequence using least squares. The objective of this paper is to examine the efficiency of the CDSSSIT in identifying the modal parameters (frequencies and mode shapes) of a stiff structure. The results show that the CDSSSIT predicts the modal parameters of stiff buildings quite accurately but is very sensitive to the location of sensors.

**Keywords:** system identification; optimal sensor placement; structural health monitoring; subspace based system identification.

---

## 1. Introduction

System identification techniques have been successfully implemented in the literature to identify the modal parameters of bridges and high rise buildings (Kohler *et al.* 2005, Safak 1993, Celebi and Safak 1992, Safak and Celebi 1992, Azarbayejani *et al.* 2009a, b, Mosallam *et al.* 2009, Cardini and DeWolf 2009). However, for stiff structures, application of the system identification techniques still is a challenge despite the advances in the electronics of health monitoring systems for the past 15 years. The Combined Deterministic Stochastic Subspace based System Identification Technique (CDSSSIT) within this context, is a powerful input-output system identification technique that is known to be always convergent, non-iterative and numerically stable (Van Overschee and De Moor 1992a, b, 1994a, b, 1995, 1996). In classical identification techniques, first the system matrices are determined and then the Kalman states are identified from these system matrices through Kalman filter (Van Overschee and De Moor 1992a, b, 1996). The CDSSSIT on the other hand, determines a Kalman state sequence from the projection of the input-output data. The state space matrices are determined subsequently from this Kalman state sequence using least squares. This is the difference between the CDSSSIT algorithms and the classical identification schemes. The objective of this paper is to search for the efficiency of the CDSSSIT in identifying the modal parameters of a stiff building and to examine the sensitivity of the technique to different sensor locations.

---

\*Corresponding author, Professor, E-mail: [gundesbakir@yahoo.com](mailto:gundesbakir@yahoo.com)

A school building in Istanbul is monitored continuously for a TUBITAK Project (Gundes Bakir 2008). Before the instrumentation of the school, the toolbox OPTISEP (OPTImal Sensor Placement (OSP)) was developed in MATLAB by the author in a previous study (Gundes Bakir 2010) which can compute the optimum sensor locations according to six alternative OSP techniques currently used in NASA for large space structures. The techniques in the toolbox are then applied on this stiff school building. The previous study showed that the Sensor Set Expansion Technique is the most suitable technique for OSP in stiff mid rise reinforced concrete buildings. However, no system identification step was involved in the previous study. Thus, it is now timely and imperative to investigate the feasibility of the application of the CDSSSIT on the response data obtained from different sensor configurations. This is the first objective of this paper. The parametric studies as well as the Monte Carlo analysis will give the crucial information regarding the validity of the previous study of the author (Gundes Bakir 2010) which compared different OSP techniques only in terms of the determinant, the trace and the condition number of the Fisher Information Matrix (FIM). A second objective of the study is to investigate whether the CDSSSIT, which is reported to be numerically stable and convergent in the literature, can also successfully identify the modal parameters (frequencies, mode shapes) of stiff mid rise reinforced concrete building type structures and whether the technique has some limitations.

In this paper, a linear dynamic analysis is carried out on the finite element (FE) model of the building and the response data is obtained from different sensor configurations. The CDSSSIT is then applied on these response data to identify the modal parameters of the structure. A Monte Carlo analysis is carried out and the identified modal parameters are then compared with the modal parameters obtained from the FE model of the structure using the average values of the relative eigenfrequency differences (RED) and the modal assurance criteria (MAC) from the Monte Carlo simulations. The overall results of the study show that the CDSSSIT is overly sensitive to the location of sensors.

## 2. The CDSSSIT

The CDSSSIT by Van Overschee and De Moor (Van Overschee and De Moor 1992a, b, 1994a, b, 1996) is explained in the following subsections.

### 2.1 The combined deterministic-stochastic model

The combined deterministic-stochastic model that will be identified is given by

$$x_{k+1} = Ax_k + Bu_k + w_k \quad (1)$$

$$y_k = Cx_k + Du_k + v_k \quad (2)$$

with

$$\mathbf{E} \left[ \begin{pmatrix} w_k \\ v_k \end{pmatrix} \begin{pmatrix} w_l^T & v_l^T \end{pmatrix} \right] = \begin{pmatrix} Q^s & S^s \\ (S^s)^T & R^s \end{pmatrix} \delta_{kl} \quad (3)$$

where  $A, Q^s \in \mathbb{R}^{n \times n}$ ,  $B \in \mathbb{R}^{n \times m}$ ,  $C \in \mathbb{R}^{l \times n}$ ,  $D \in \mathbb{R}^{l \times m}$ ,  $S^s \in \mathbb{R}^{n \times l}$  and  $R^s \in \mathbb{R}^{l \times l}$ . The vectors  $v_k \in \mathbb{R}^{l \times 1}$  and  $w_k \in \mathbb{R}^{n \times 1}$  are unmeasurable, Gaussian distributed zero mean white noise vector sequences,  $l$  is

the number of outputs,  $m$  is the number of inputs and  $A, B, C, D$  are the system matrices of the state space model. This system is subdivided into the deterministic and the stochastic parts. The stochastic part is denoted by a superscript  $s$  and the deterministic part is denoted by a superscript  $d$ . The deterministic and the stochastic models can be expressed as

$$x_{k+1}^d = Ax_k^d + Bu_k \tag{4}$$

$$y_k^d = Cx_k^d + Du_k \tag{5}$$

$$x_{k+1}^s = Ax_k^s + w_k \tag{6}$$

$$y_k^s = Cx_k^s + v_k \tag{7}$$

### 2.2 Construction of the block Hankel matrices

Block Hankel matrices are constructed from the input and output data. The subscripts of the input block Hankel matrix  $U$  in the following two equations represent the first and the last element of the first column. Similarly,  $U_{0|i-1}$  is denoted by  $U_p$  and  $U_{i|2i-1}$  by  $U_f$  where the subscripts  $p$  and  $f$  denote the past and the future, respectively,  $i$  is the number of block rows,  $j$  is the number of columns of the block Hankel matrices. From a statistical point of view  $j$  should be much larger than  $i$ . To ensure that all the samples are used,  $j$  is taken as equal to  $s - 2i + 1$ , where  $s$  is the number of samples of the measurement. The output block Hankel matrices  $Y_{0|2i-1}, Y_p, Y_f, Y_p^+, Y_f^-$  are defined similar to Eqs. (8) and (9). A block Hankel matrix  $W_{0|i-1}$  consisting of inputs and outputs is also defined in Eq. (10).

$$U_{0|2i-1} = \begin{pmatrix} u_0 & u_1 & \dots & u_{j-1} \\ u_1 & u_2 & \dots & u_j \\ \dots & \dots & \dots & \dots \\ u_{i-1} & u_i & \dots & u_{i+j-2} \\ u_i & u_{i+1} & \dots & u_{i+j-1} \\ u_{i+1} & u_{i+2} & \dots & u_{i+j} \\ \dots & \dots & \dots & \dots \\ u_{2i-1} & u_{2i} & \dots & u_{2i+j-2} \end{pmatrix} = \begin{pmatrix} U_{0|i-1} \\ U_{i|2i-1} \end{pmatrix} = \begin{pmatrix} U_p \\ U_f \end{pmatrix} \tag{8}$$

$$U_{i|2i-1} = \begin{pmatrix} u_0 & u_1 & \dots & u_{j-1} \\ u_1 & u_2 & \dots & u_j \\ \dots & \dots & \dots & \dots \\ u_i & u_{i+1} & \dots & u_{i+j-1} \\ u_{i+1} & u_{i+2} & \dots & u_{i+j} \\ \dots & \dots & \dots & \dots \\ u_{2i-1} & u_{2i} & \dots & u_{2i+j-2} \end{pmatrix} = \begin{pmatrix} U_{0|i} \\ U_{i+1|2i-1} \end{pmatrix} = \begin{pmatrix} U_p^+ \\ U_f^- \end{pmatrix} \tag{9}$$

$$W_{0|i-1} = \begin{pmatrix} U_{0|i-1} \\ Y_{0|i-1} \end{pmatrix} = \begin{pmatrix} U_p \\ Y_p \end{pmatrix} = W_p \tag{10}$$

### 2.3 Combined deterministic stochastic subspace system identification

The orthogonal and the oblique projections are two extensively used geometrical tools in subspace based system identification. The orthogonal projection is denoted by the operator  $\Pi_F$  that projects the row space of the matrix onto the row space of the matrix  $F$  as

$$\Pi_F = F^T(FF^T)^\dagger F \quad (11)$$

where  $(\bullet)^\dagger$  defines the Moore-Penrose pseudo-inverse of the matrix  $(\bullet)$ .

$$E/\mathbf{F} = E\Pi_F = EF^T(FF^T)^\dagger F \quad (12)$$

It should be noted that  $F$  in the above equation is written in bold face in order to indicate that the result of the above operation  $E/\mathbf{F}$  is in the row space of  $F$ . The oblique projection of the row space of  $E$  along the row space of  $F$  on the row space of  $G$  is defined as follows

$$E/{}_F\mathbf{G} = [E/\mathbf{F}^\perp][G/\mathbf{F}^\perp]^\dagger G \quad (13)$$

where

$$E/\mathbf{F}^\perp = E\Pi_{F^\perp} \quad (14)$$

$$\Pi_{F^\perp} = I_j - \Pi_F \quad (15)$$

In the combined deterministic stochastic subspace based system identification technique, the oblique and the orthogonal projections given below are computed first

$$O_i = Y_f /_{U_f} \mathbf{W}_p \quad (16)$$

$$Z_i = Y_f / \begin{pmatrix} \mathbf{W}_p \\ \mathbf{U}_f \end{pmatrix} \quad (17)$$

$$Z_{i+1} = Y_{f'} / \begin{pmatrix} \mathbf{W}_p^+ \\ \mathbf{U}_f^- \end{pmatrix} \quad (18)$$

where

$$\mathbf{W}_p^+ = \begin{pmatrix} \mathbf{U}_p^+ \\ \mathbf{Y}_p^+ \end{pmatrix} \quad (19)$$

The singular value decomposition of the weighted oblique projection  $W_1 O_i W_2 = USV^T$  is calculated next.

$$W_1 O_i W_2 = (U_1 U_2) \begin{pmatrix} S_1 & 0 \\ 0 & 0 \end{pmatrix} \begin{pmatrix} V_1^T \\ V_2^T \end{pmatrix} = U_1 S_1 V_1^T \quad (20)$$

where  $U = (U_1 U_2)$  and  $V = (V_1 V_2)$  are the orthonormal matrices (not to be confused with the notation  $U$  used for the input block Hankel matrices) and  $S$  is a diagonal matrix that contains the singular values in the diagonal. The user defined weighting matrices  $W_1 \in \mathbb{R}^{l_i \times l_i}$  and  $W_2 \in \mathbb{R}^{j \times j}$  are such that  $W_1$  is of full rank and  $rank(W_p) = rank(W_p W_2)$ .

The extended observability  $\Gamma_i$  and the extended observability matrices without the last  $l$  rows represented by  $\underline{\Gamma}_i$  are computed from

$$\Gamma_i = W_1^{-1} U_1 S_1^{1/2} \quad (21)$$

$$\Gamma_{i-1} = \underline{\Gamma}_i \quad (22)$$

The following equation is solved for  $A$ ,  $C$  and  $K$

$$\begin{pmatrix} \Gamma_{i-1}^\dagger Z_{i+1} \\ Y_{i|i} \end{pmatrix} = \begin{pmatrix} A \\ C \end{pmatrix} \Gamma_i^\dagger Z_i + K U_f + \begin{pmatrix} \rho_w \\ \rho_v \end{pmatrix} \quad (23)$$

The matrices  $L$ ,  $M$  and  $K$  are defined as

$$L = \begin{pmatrix} A \\ C \end{pmatrix} \Gamma_i^\dagger = \begin{pmatrix} L_{1|1} & L_{1|2} & \dots & L_{1|i} \\ L_{2|1} & L_{2|2} & \dots & L_{2|i} \end{pmatrix} \in \mathbb{R}^{(n+l) \times li} \quad (24)$$

$$M = \Gamma_{i-1}^\dagger = (M_1 \ M_2 \ \dots \ M_{i-1}) \in \mathbb{R}^{n \times l(i-1)} \quad (25)$$

$$K = \begin{pmatrix} K_{1|1} & K_{1|2} & \dots & K_{1|i} \\ K_{2|1} & K_{2|2} & \dots & K_{2|i} \end{pmatrix} \quad (26)$$

where  $L_{1|k}, M_k \in \mathbb{R}^{n \times l}, K_{1|k} \in \mathbb{R}^{n \times m}, L_{2|k} \in \mathbb{R}^{l \times l}$  and  $K_{2|k} \in \mathbb{R}^{l \times m}$ . The state space system matrices  $B$  and  $D$  are calculated from the following equations given  $K, A, C, \Gamma_i, \Gamma_{i-1}$  as

$$\begin{pmatrix} K_{1|1} \\ \vdots \\ K_{1|i} \\ K_{2|2} \\ \vdots \\ K_{2|i} \end{pmatrix} = N \begin{pmatrix} D \\ B \end{pmatrix} \quad (27)$$

$$N = \begin{bmatrix} -L_{1|1} & M_1 - L_{1|2} & \dots & M_{i-2} - L_{1|i-1} & M_{i-1} - L_{1|i} \\ M_1 - L_{1|2} & M_2 - L_{1|3} & \dots & M_{i-1} - L_{1|i} & 0 \\ M_2 - L_{1|3} & M_3 - L_{1|4} & \dots & 0 & 0 \\ \dots & \dots & \dots & \dots & \dots \\ M_{i-1} - L_{1|i} & 0 & \dots & 0 & 0 \\ I_l - L_{2|1} & -L_{2|2} & \dots & -L_{2|i-1} & -L_{2|i} \\ -L_{2|2} & -L_{2|3} & \dots & -L_{2|i} & 0 \\ -L_{2|3} & -L_{2|4} & \dots & 0 & 0 \\ \dots & \dots & \dots & \dots & \dots \\ -L_{2|i} & 0 & \dots & 0 & 0 \end{bmatrix} \times \begin{pmatrix} I_l & 0 \\ 0 & \Gamma_{i-1} \end{pmatrix} \quad (28)$$

The matrices  $Q$ ,  $S$  and  $R$  can be computed from the residuals  $\rho_w$  and  $\rho_v$  as

$$\begin{pmatrix} Q & S \\ S^T & R \end{pmatrix} = \mathbf{E}_j \begin{bmatrix} \rho_w \\ \rho_w^T & \rho_v^T \end{bmatrix} \quad (29)$$

#### 2.4 Derivation of the eigenfrequencies and mode shapes from the state space system matrices

The system matrix  $A$  can be decomposed as (Peeters 2000)

$$A = \psi \Lambda_d \psi^{-1} \quad (30)$$

where  $\psi \in C^{n \times n}$  is the eigenvector matrix and  $\Lambda_d \in C^{n \times n}$  is a diagonal matrix that contains the discrete time eigenvalues  $\mu_i$ . The eigenfrequencies are calculated from

$$\lambda_i = \frac{\ln(\mu_i)}{\Delta t} \quad (31)$$

where  $\lambda_i$  denotes the continuous time eigenvalues and  $\Delta t$  is the sampling time. The mode shapes  $V$  are computed from

$$V = C \psi \quad (32)$$

### 3. The optimal sensor placement techniques

Six different OSP techniques are implemented in the toolbox OPTISEP developed by the author. These OSP techniques are initially developed for OSP in large space structures such as space shuttles, satellites or other types of large space structures in NASA. Different techniques that are incorporated in the toolbox are the Effective Independence Technique (EFIT) (Kammer 1991, Kammer and Tinker 2004), Optimal Driving Point Technique (ODPT) (Imamovic 1998, Doebling 1996), Non-Optimal Driving Point Technique (NODPT) (Imamovic 1998), Effective Independence-Driving Point Residue Technique (EFI-DPRT), the Singular Value Decomposition based Technique (SVD-OSPT) by Kim and Park (1997) and the Sensor Set Expansion Technique (SSET) by Kammer (2005). Since the previous study of the author (Gundes Bakir 2010) has shown that the SVD-OSPT and the EFIT gives identical sensor configurations, the SVD-OSPT will not be further considered in this paper. The rest of the techniques will be very briefly explained here and the detailed presentations of the techniques as well as the toolbox OPTISEP developed by the author can be found elsewhere (Gundes Bakir 2010) and is out of the scope of this paper.

#### 3.1 The effective independence technique (EFIT)

The effective independence value  $E_i$  associated with the  $i$ th sensor given by the following equation is computed first in the EFIT. The  $E_i$  is the percentage of decrease in the determinant of the FIM if the  $i$ th sensor is deleted from the candidate set.

$$E_i = \phi_{si} Q^{-1} \phi_{si}^T \quad (33)$$

where

$$Q = \sum_{i=1}^{n_c} \phi_{si}^T \phi_{si} = \sum_{i=1}^{n_c} Q_i \quad (34)$$

$\phi_{si}$  is the  $i$ th row of the target mode participation matrix corresponding to the  $i$ th candidate sensor location and  $n_c$  is the number of candidate sensors. The algorithm in an iterative way calculates the effective independence value that corresponds to every candidate sensor location and then deletes the one that has the smallest contribution until the number of the candidate sensor locations are equal to the available number of sensors. The value of  $E_i$  is between 0 and 1. If this value is equal to 1 for a sensor location, then that location is crucial and should not be deleted from the candidate sensor locations. If it is 0, then that sensor location has no contribution to the signal strength or spatial independence.

### 3.2 The effective independence driving point residue technique (EFI-DPRT)

It has been argued in the literature (Imamovic 1998) that with the EFIT, sensor locations with low energy content can also be selected. This is overcome in the EFI-DPRT by multiplying the effective independence value for each candidate sensor location by the corresponding driving point residue coefficient given by

$$DPR_i = \sum_{j=1}^N \frac{\Phi_{ij}^2}{\omega_j} \quad (35)$$

where  $\omega_j$  is the  $j$ th target mode frequency. Consequently, the effective independence value for the EFI-DPRT can be computed as

$$E_i^{EFI-DPRT} = E_i DPR_i \quad (36)$$

### 3.3 Optimum driving point based technique (ODPT)

In the ODP technique, the ODP parameter is computed which can be expressed as

$$ODP(i) = \prod_{r=1}^k \|\phi_{i,r}\| \quad (37)$$

The idea is to detect the nodal points in order to prevent the sensors to be located in these regions.

### 3.4 Non-optimum driving point based technique (NODPT)

This is an energy based algorithm that uses the NODP parameter which is defined as

$$NODP(i) = \min_r (\|\phi_{i,r}\|) \quad (38)$$

In this methodology, the sensor locations with the lowest NODP parameters are deleted from the candidate sensor locations in an iterative way.

### 3.5 Sensor set expansion technique (SSET)

SSET developed by Kammer (2005) iteratively expands an initial set of sensors to the desired number of sensors in contrast to the above-mentioned techniques which decrease the initial set of candidate sensor locations to the available number of sensors. The method not only results in a dramatic decrease in the computational time but also allows a test engineer to specify a set of locations that they absolutely want to keep in the final sensor configuration. The expert engineers can determine an initial set of sensor locations and then expand this initial set to the desired number of sensors in an optimal way. The method essentially is based on maximizing the determinant of the target mode information matrix. Maximizing the determinant, increases both the target mode signal strength and the linear independence. There are two different cases that must be examined when using the technique. These are when the initial node set renders target mode shapes linearly independent and when the initial node set renders target mode shapes linearly dependent. The details of the technique can be found in Kammer (2005). The SSET is originally developed for triaxial sensors. However, in this study, it is implemented slightly differently so that it can also be applied on uniaxial sensors with the same logic of expanding an initial predetermined set of sensors to the available number of sensors.

## 4. The instrumented school building

The instrumented building is a five storey structure with one basement as shown in Fig. 1 and is located in the Kadikoy district of Istanbul on the Asian side.

The first four mode shapes of the frame are shown in Figs. 2, 3, 4 and 5.

The modal frequencies are given in Table 1. One of the considerations in this study is the typical structural design of the school building. The structure is substantially stiff in the short direction and relatively stiff in the long direction. Therefore, one of the other aims of this paper



Fig. 1 The instrumented school building (website of the instrumented building, 2009)

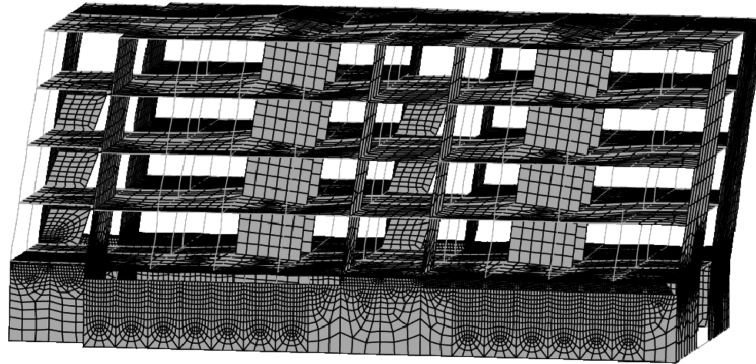


Fig. 2 The first vibration mode (the first bending mode in the longitudinal direction)

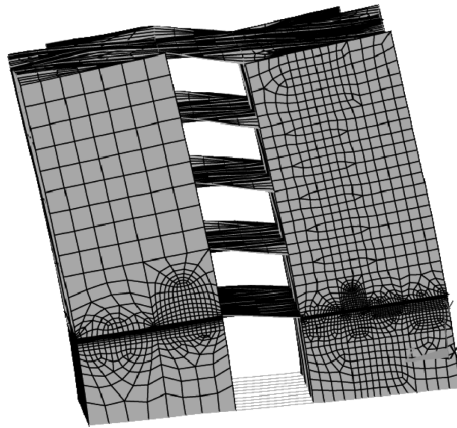


Fig. 3 The second vibration mode (the first bending mode in the transversal direction)

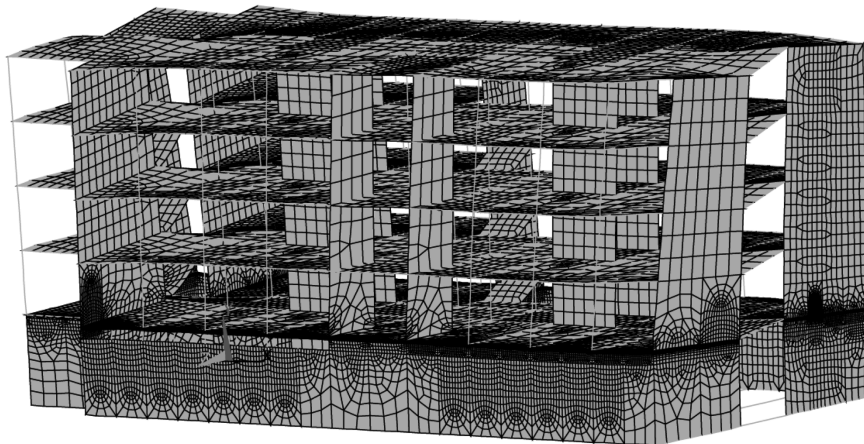


Fig. 4 The third vibration mode (the torsional mode)

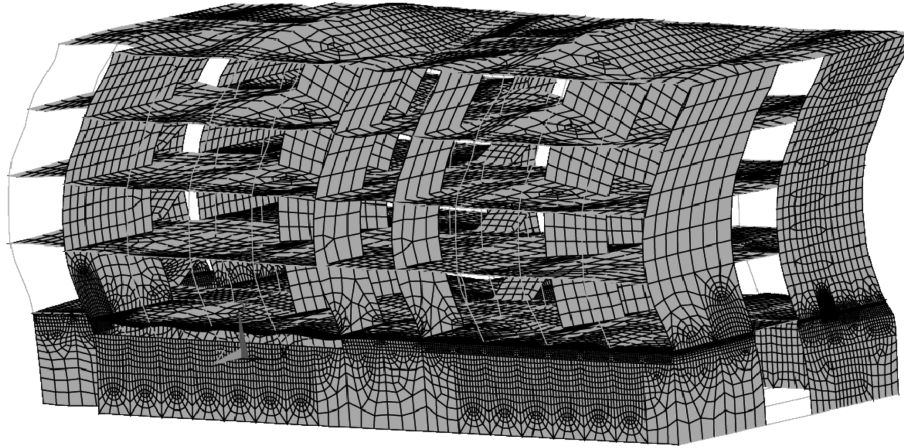


Fig. 5 The fourth vibration mode (the second bending mode in the longitudinal direction)

Table 1 Modal frequencies

Number	Frequency (Hz)	Mode type
1	2.62	First bending mode in the $z$ direction
2	4.84	First bending mode in the $x$ direction
3	5.91	First torsion mode
4	10.007	Second bending mode in the $z$ direction
5-12	10.133	Local modes of the ground storey beams

is to answer the question whether the CDSSSIT will successfully identify the global modes in such a stiff structure.

## 5. Final optimal sensor configuration in the school building

The OSP toolbox OPTISEP has been applied on the stiff school building in a previous study of the author (Gundes Bakir 2010). The resulting sensor configurations are shown in Figs. 6 and 7. The techniques are compared in terms of the determinant, the trace and the condition number of the FIM in the previous paper. The results showed that the SSET gives the best results among all the six different techniques. However, no identification step is involved in the afore-mentioned study. In this stage of the project, the CDSSSIT will be implemented when collecting real time data from this building for identifying the modal parameters. Thus, it is now timely to investigate whether the modal parameters are identified successfully with the CDSSSIT. In this paper, several parametric studies and Monte Carlo simulations are carried out to determine the best OSP technique that would give the best eigenfrequency and mode shape estimates when the CDSSSIT is applied on the response data from this structure.

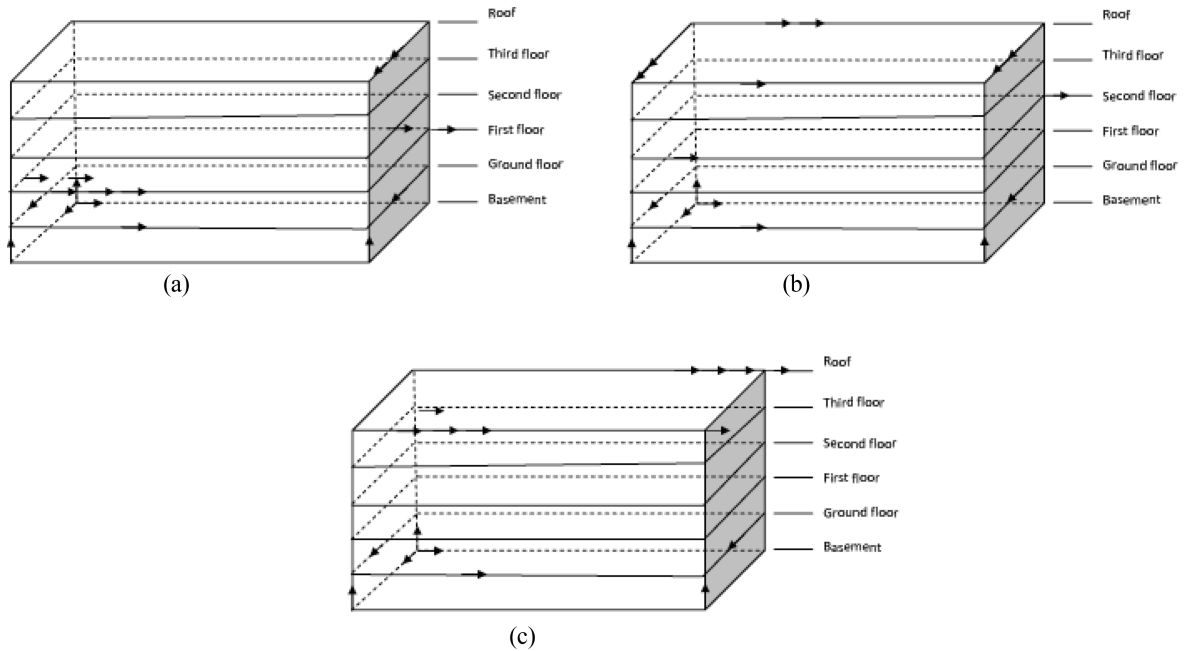


Fig. 6 Final sensor configurations according to (a) NODPT (b) EFIT and SVD-OSPT (c) ODP method (Gundes Bakir 2010)

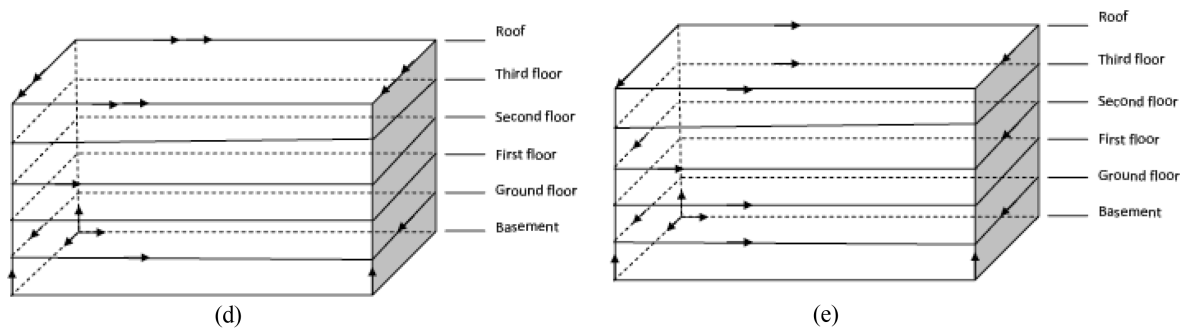


Fig. 7 Final sensor configurations according to (d) EFI-DPRT, (e) SSET (Gundes Bakir 2010)

## 6. Implementation of CDSSIT and the parametric studies

A linear dynamic analysis is carried out on the stiff school building and the response data is obtained from different sensor configurations. The dynamic excitation load is white noise Gaussian with 4096 samples of  $dt = 0.005$  sec. The total excitation period is 20.475 sec. The structure is excited in both horizontal directions. The response data is obtained from the assumed sensor configurations according to the 6 different techniques. The CDSSIT, specifically, the com-alt algorithm (Van Overschee and De Moor 1996) is then successfully applied on these response data to identify the modal parameters of the structure first for the case without noise and then for a noise to

signal ratio (NSR) of 10% for each sensor configuration. These are then compared with the modal parameters obtained from the FE model of the structure using RED and MAC. A Monte Carlo analysis of 40 runs is carried out in order to investigate the robustness of the techniques in the presence of noise and the average results are plotted. This is a feasibility study for determining the most efficient and the most accurate modal parameters from the instrumented school building using the CDSSSIT.

The RED obtained from CDSSSIT according to different sensor configurations for the cases without noise and with a NSR of 10% are given in Figs. 8-17.

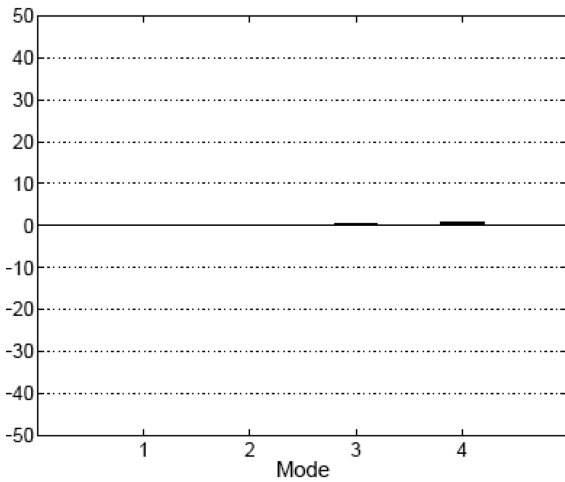


Fig. 8 The RED obtained with CDSSSIT and SSET without noise (average of the Monte Carlo simulations)

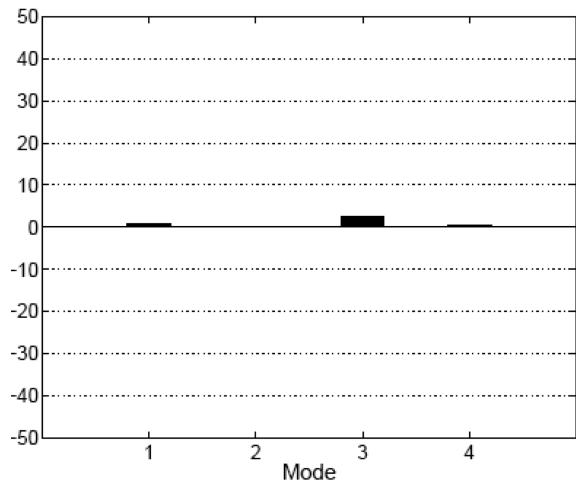


Fig. 9 The RED obtained with CDSSSIT and SSET for a NSR of 10% (average of the Monte Carlo simulations)

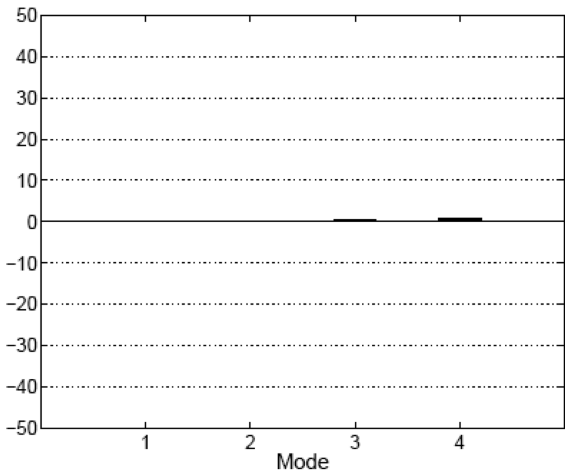


Fig. 10 The RED obtained with EFIT and CDSSSIT without noise (average of the Monte Carlo simulations)

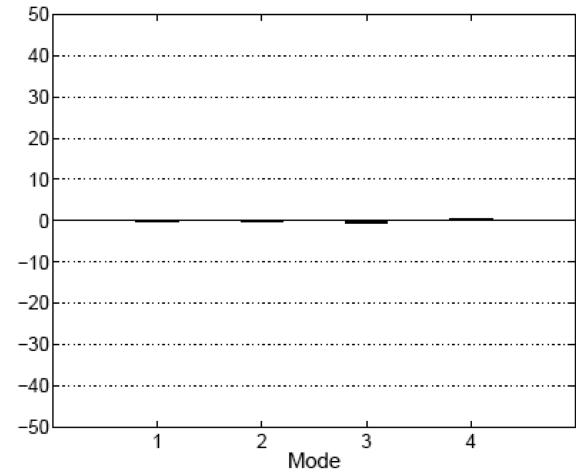


Fig. 11 The RED obtained with EFIT and CDSSSIT for a NSR of 10% (average of the Monte Carlo simulations)

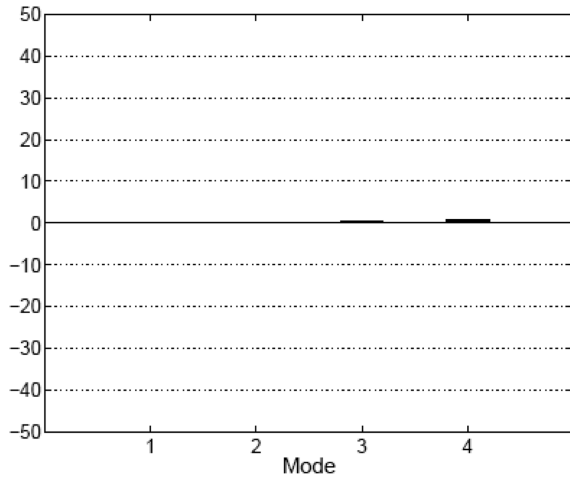


Fig. 12 The RED obtained from EFI-DPRT and CDSSSIT without noise (average of the Monte Carlo simulations)

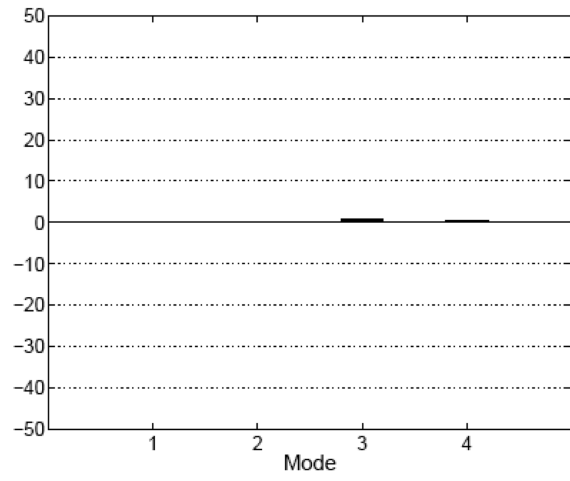


Fig. 13 The RED obtained from EFI-DPRT and CDSSSIT for a NSR of 10% (average of the Monte Carlo simulations)

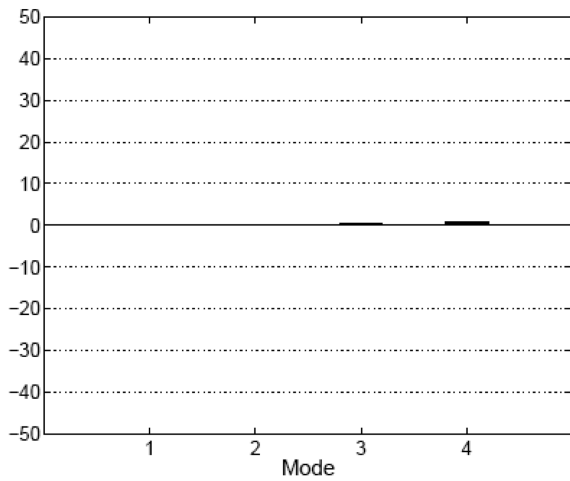


Fig. 14 The RED obtained using CDSSSIT and ODPT without noise (average of the Monte Carlo simulations)

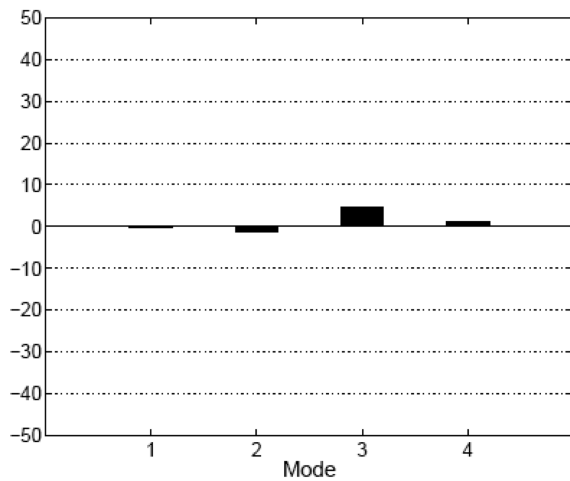


Fig. 15 The RED obtained using CDSSSIT and ODPT with a NSR of 10% (average of the Monte Carlo simulations)

The average MAC obtained by the CDSSSIT from Monte Carlo simulations according to different sensor configurations for the cases without noise and with a NSR of 10% are given in Figs. 18-27.

## 7. Results and discussion

The results show the average of the Monte Carlo runs and demonstrate clearly that with all of the

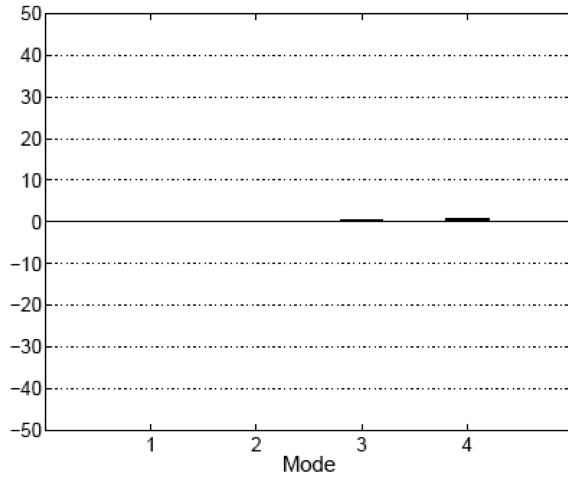


Fig. 16 The RED obtained from CDSSSIT and NODPT without noise (average of the Monte Carlo simulations)

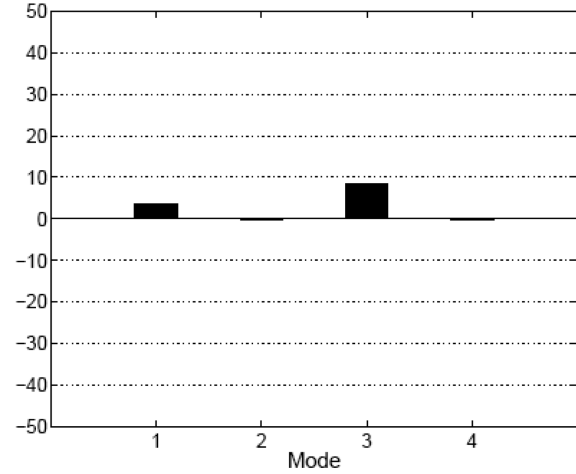


Fig. 17 The RED obtained from CDSSSIT and NODPT for a NSR of 10% (average of the Monte Carlo simulations)

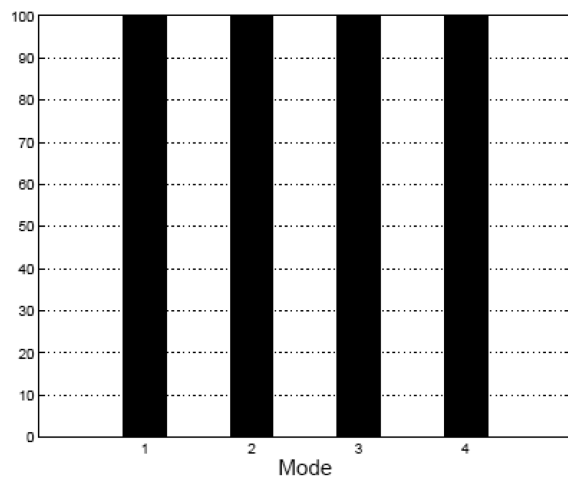


Fig. 18 The MAC from CDSSSIT and SSET without noise (average of the Monte Carlo simulations)

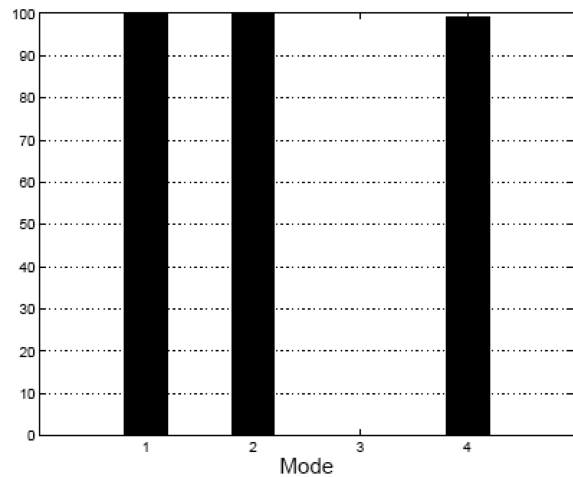


Fig. 19 The MAC from CDSSSIT and SSET for a NSR of 10% (average of the Monte Carlo simulations)

OSP techniques, the eigenfrequencies of this stiff structure can be adequately identified using CDSSSIT. However, with none of the OSP configurations except for the SSET, the mode shapes of the structure can be adequately identified. This is even true without noise. For the case without noise, the MAC values using SSET in combination with the CDSSSIT are substantially high whereas the mode shapes can not be adequately captured using other OSP configurations. It is also apparent that even for the case with a NSR of 10%, the first, the second and the fourth modes are very accurately identified using the SSET in combination with the CDSSSIT. There is only a problem with the torsional mode. This can be expected as the structure was too stiff in the short

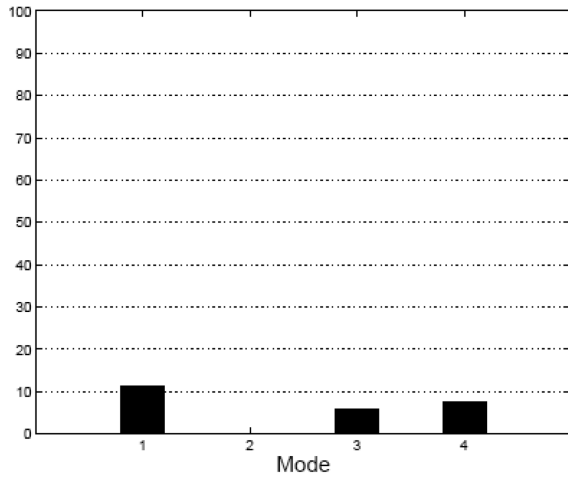


Fig. 20 The MAC from the EFIT without noise (average of the Monte Carlo simulations)

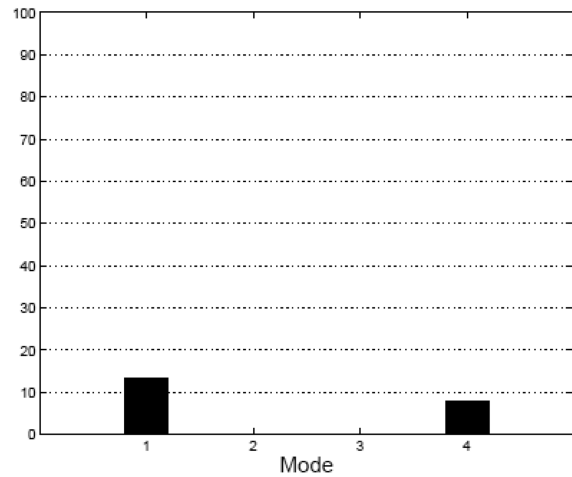


Fig. 21 The MAC from the EFIT and CDSSSIT for a NSR of 10% (average of the Monte Carlo simulations)

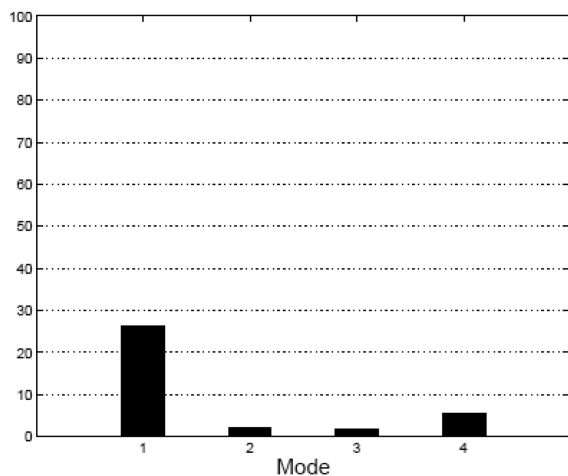


Fig. 22 The MAC from EFI-DPRT and CDSSSIT without noise (average of the Monte Carlo simulations)

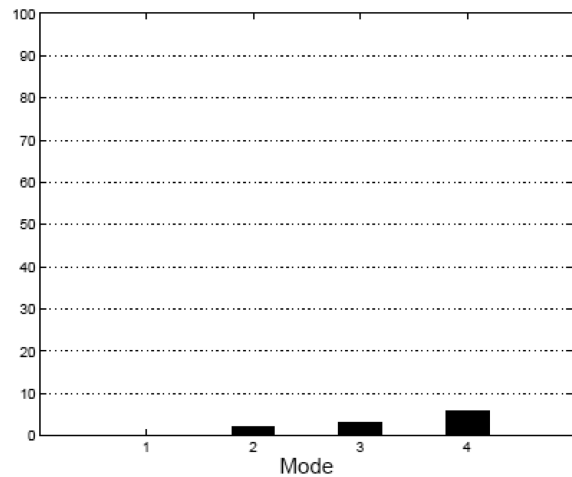


Fig. 23 The MAC from EFI-DPRT and CDSSSIT for a NSR of 10% (average of the Monte Carlo simulations)

direction and was not excited in all directions in the dynamic analysis. These may be the reasons behind the relatively lower MAC values for the torsional mode.

As mentioned above, the mode shapes can not be adequately identified with CDSSSIT for sensor configurations computed according to the other techniques than the SSET. The reason may be the following: When the sensor configuration computed according to the NODPT is investigated in detail, it is apparent that the sensors are concentrated in the lower stories at the left hand side and only 2 sensors in the short direction are present in the roof. In the EFIT, ODPT and EFI-DPRT, the sensors are mainly located in the upper stories. In the sensor distribution obtained from ODPT, there

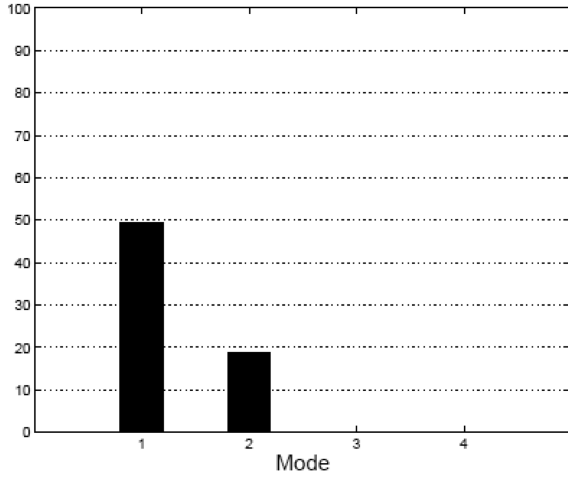


Fig. 24 The MAC from CDSSSIT and ODPT without noise (average of the Monte Carlo simulations)

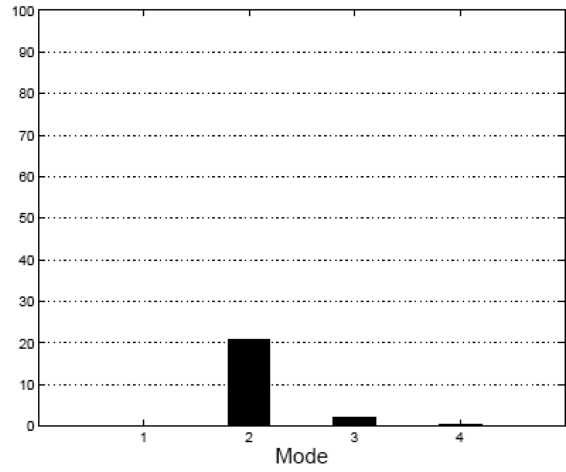


Fig. 25 The MAC from CDSSSIT and ODPT for a NSR of 10% (average of the Monte Carlo simulations)

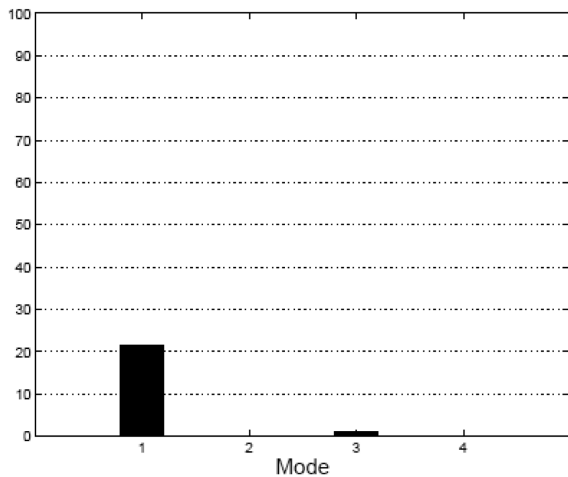


Fig. 26 The MAC from CDSSSIT and NODPT without noise (average of the Monte Carlo simulations)

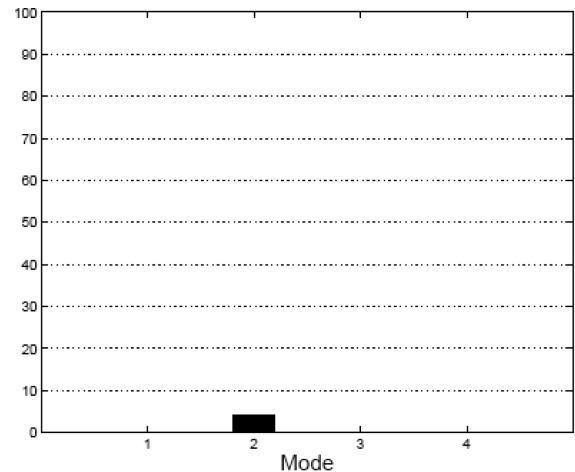


Fig. 27 The MAC from CDSSSIT and NODPT for a NSR of 10% (average of the Monte Carlo simulations)

is no single sensor in the short direction in the 2nd, 3rd, 4th and the 5th stories. If the sensor configuration with the SSET is investigated on the other hand, it becomes apparent that the sensors are distributed homogeneously throughout the structure.

The overall results of the parametric studies show that the best estimates are obtained from the CDSSSIT when the sensor configuration is computed according to the SSET but it is also apparent that the CDSSSIT falls short of accurately identifying the mode shapes of such a stiff structure when other techniques are used for OSP. The parametric studies also reveal the vulnerability of the CDSSSIT to the presence of noise in measurements.

## 8. Conclusions

It is relatively easier to identify the modal parameters of flexible structures from the response data. However, for stiff structures, application of the system identification techniques becomes a challenge. This paper investigates the feasibility of the application of the CDSSSIT on the response data obtained from stiff building type structures for the identification of modal parameters. The use of this technique is important as it is known to be always convergent and numerically stable. A Monte Carlo analysis is carried out and the average results from simulations are compared in terms of the RED as well as the MAC. The results of these parametric studies show that the CDSSSIT predicts the modal parameters of stiff structures quite accurately but is sensitive to the location of sensors and the best results can be obtained from the CDSSSIT if it is used in combination with the OSP method SSET. It is also apparent that the CDSSSIT is vulnerable to the presence of noise in measurements and this limitation of the technique ought to be considered when it is applied on stiff mid rise building type structures.

## Acknowledgements

This study is carried out in the framework of the TUBITAK project 107M573 for which the author is the promotor. This support is acknowledged here.

## References

- Azarbayejani, M., El-Osery A.I. and Taha, M.M.R. (2009a), "Entropy-based optimal sensor networks for structural health monitoring of a cable-stayed bridge", *Smart Struct. Syst.*, **5**(4), 369-379.
- Azarbayejani, M., El-Osery, A.I. and Taha, M.M.R. (2009b), "Condition assessment of reinforced concrete bridges using structural health monitoring techniques - A case study", *Smart Struct. Syst.*, **5**(4), 381-395.
- Gundes Bakir, P. (2008), TUBITAK Project No:107M573, *Damage Identification in Existing Buildings Using Real Time System Identification Techniques and Finite Element Model Updating*, ITU, Istanbul, Turkey.
- Gundes Bakir, P. (2010), "Evaluation of optimal sensor placement techniques in buildings", *Math. Comput. Appl.* (accepted for publication)
- Cardini, A.J. and DeWolf, J.T. (2009), "Long-term structural health monitoring of a multi-girder steel composite bridge using strain data", *Struct. Hlth. Monit.*, **8**(1), 47-58.
- Celebi, M. and Safak, E. (1992), "Seismic response of Pasific Park Plaza, 1. data and preliminary analysis", *J. Struct. Eng.-ASCE*, **118**(6), 1547-1592.
- Doebling, S.W. (1996), "Measurement of structural flexibility matrices for experiments with incomplete reciprocity", PhD Thesis, Colorado University, USA.
- Imamovic, N. (1998), "Model validation of large finite element model using test data", PhD Thesis, Imperial College, London, UK.
- Kammer, D.C. (1991), "Sensor placement for on-orbit modal identification and correlation of large space structures", *J. Guid. Control Dynam.*, **14**(2), 251-259.
- Kammer, D.C. and Tinker, M.L. (2004), "Optimal placement of triaxial accelerometers for modal vibration tests", *Mech. Syst. Signal Pr.*, **18**, 29-41.
- Kammer, D.C. (2005), "Sensor set expansion for modal vibration testing", *Mech. Syst. Signal Pr.*, **19**(4), 700-716.
- Kim, H.B. and Park, Y.S. (1997), "Sensor placement guide for structural joint stiffness model improvement", *Mech. Syst. Signal Pr.*, **11**(5), 651-672.

- Kohler, M.D., Davis, P.M. and Safak, E. (2005), "Earthquake and ambient vibration monitoring of the steel frame UCLA factor building", *Earthq. Spectra*, **21**(3), 715-736.
- Mosallam, A., Miraj, R. and Abdi, F. (2009), "Diagnostic/prognostic health monitoring system and evaluation of a composite bridge", *Smart Struct. Syst.*, **5**(4), 397-413.
- Peeters, B. (2000), "System identification and damage detection in civil engineering", PhD Thesis, Department of Civil Engineering, Katholieke Universiteit Leuven, Belgium.
- Safak, E. and Celebi, M. (1992), "Seismic response of Pasific Park Plaza, 2. system identification", *J. Struct. Eng.-ASCE*, **118**(6), 1566-1589.
- Safak, E. (1993), "Response of a 42 storey steel-frame building to the M(s)=7.1 Lome-Prieta earthquake", *Eng. Struct.*, **15**(6), 403-421.
- Van Overschee, P. and De Moor, B. (1992a), "Subspace algorithms for the identification of combined deterministic-stochastic systems", ESAT/SISTA Report 1992-10, Katholieke Universiteit Leuven, Department of Electrical Engineering, Belgium.
- Van Overschee, P. and De Moor, B. (1992b), "Two subspace algorithms for the identification of combined deterministic stochastic systems", *Proceedings of the 31st IEEE Conference on Decision and Control*, Tucson, USA, December.
- Van Overschee, P. and De Moor, B. (1994a), "A unifying theorem for three subspace system identification algorithms", *Proceedings of the SYSID '94*, Copenhagen, Denmark, July.
- Van Overschee, P. and De Moor, B. (1994b), "Subspace algorithms for the identification of combined deterministic-stochastic systems", *Automatica, Special issue on Statistical Signal Processing and Control*, **30**(1), 75-93.
- Van Overschee, P. and De Moor, B. (1995), "A unifying theorem for three subspace system identification algorithms", *Automatica*, **31**(12), 1877-1883.
- Van Overschee, P. and De Moor, B. (1996), *Subspace Identification for Linear Systems*, Kluwer Academic Publishers, Massachusetts, USA.
- Website of the Instrumented Building (2007), Available at: [www.erenkoy.k12.tr/](http://www.erenkoy.k12.tr/).